Transfusion Medicine and Hemotherapy

Research Article

Transfus Med Hemother 2022;49:346–356
DOI: 10.1159/000524849

Received: September 1, 2021
Accepted: May 1, 2022
Published online: July 5, 2022

Preliminary Study of Genome-Wide Association Identified Novel Susceptibility Genes for Hemorheological Indexes in a Chinese Population

Yuxiao Sun[a, b, c, d] Zhaoyun Cheng[a, b, c] Zhiping Guo[a, b, c, d] Guoyou Dai[a, b, c, d]
Yongqiang Li[a, b, c] Yan Chen[a, b, c] Ruigang Xie[a, b, c] Xianqing Wang[a, b, c]
Mingxia Cui[b, c] Guoqing Lu[a, b, c] Aifeng Wang[b, c] Chuanyu Gao[a, b, c, d]

[a]Department of Cardiology, Henan Provincial People's Hospital, Zhengzhou, PR China; [b]FuWai Central China Cardiovascular Hospital, Zhengzhou, PR China; [c]People's Hospital of Zhengzhou University, Zhengzhou, PR China; [d]Henan Provincial Key Lab for Control of Coronary Heart Disease, Zhengzhou, PR China

Keywords

Genome-wide association studies · Hemorheological traits · Healthy Chinese Han population · Applied Biosystems Axiom™ Precision Medicine Diversity Array · Gene

Abstract

Background: Genome-wide association studies for various hemorheological characteristics have not been reported. We aimed to identify genetic loci associated with hemorheological indexes in a cohort of healthy Chinese Han individuals. ***Methods:*** Genotyping was performed using Applied Biosystems Axiom™ Precision Medicine Diversity Array in 838 individuals, and 6,423,076 single nucleotide polymorphisms were available for genotyping. The relations were examined in an additive genetic model using mixed linear regression and combined with identical by descent matrix. ***Results:*** We identified 38 genetic loci ($p < 5 \times 10^{-6}$) related to hemorheological traits. In which, *LOC102724502-OLIG2* rs28371438 was related to the levels of nd30 ($p = 8.58 \times 10^{-07}$), nd300 ($p = 1.89 \times 10^{-06}$), erythrocyte rigidity ($p = 1.29 \times 10^{-06}$), assigned viscosity ($p = 6.20 \times 10^{-08}$) and whole blood high cut relative ($p = 7.30 \times 10^{-08}$). The association of *STK32B* rs4689231 for nd30 ($p = 3.85 \times 10^{-06}$) and nd300 ($p = 2.94 \times 10^{-06}$) and *GTSCR1*-LINC01541 rs11661911 for erythrocyte rigidity ($p = 9.93 \times 10^{-09}$) and whole blood high cut relative ($p = 2.09 \times 10^{-07}$) was found. *USP25-MIR99AHG* rs1297329 was associated with erythrocyte rigidity ($p = 1.81 \times 10^{-06}$) and erythrocyte deformation ($p = 1.14 \times 10^{-06}$). Moreover, the association of *TMEM232-SLC25A46* rs3985087 and *LINC00470-MET-TL4* rs9966987 for fibrinogen ($p = 1.31 \times 10^{-06}$ and $p = 4.29 \times 10^{-07}$) and plasma viscosity ($p = 1.01 \times 10^{-06}$ and $p = 4.59 \times 10^{-07}$) was found. ***Conclusion:*** These findings may represent biological candidates for hemorheological indexes and contribute to hemorheological study.

Introduction

Most metabolic diseases are always accompanied by disorders of blood rheology, such as increased blood and plasma viscosity, decreased red blood cell deformability, and increased cell aggregation [1, 2]. Hemorheology, the study of deformation and blood flow, has more focused on the deformation and aggregation of erythrocytes since erythrocytes are the main components in blood [3–5]. Blood viscosity and erythrocytes deformability are the main factors for maintaining and regulating microcirculation. Blood and plasma viscosity are risk factors for atherosclerosis; and erythrocytes rheological changes, such as erythrocytes rigidity, have been observed in patients with hypertension, diabetes mellitus, and obesity [6–8]. Caprari et al. [1] reported that the hemorheological characteristics of SCA subjects showed high blood viscosity,

Karger@karger.com
www.karger.com/tmh

Correspondence to:
Chuanyu Gao, gaocy6802@163.com

Table 1. Characteristics of samples used in the GWAS

Characteristics	*N*/median (IQR)
n	838
Age, years	44.00 (36.00–50.00)
Female, *n* (%)	413 (49.3)
BMI, kg/m^2	23.53 (21.22–25.95)
nd1, mPas	20.51 (18.38–22.91)
nd30, mPas	5.43 (4.86–6.08)
nd300, mPas	4.14 (3.69–4.60)
Relative index of whole blood hyposectomy	14.85 (13.13–16.48)
Erythrocyte aggregation index	4.92 (4.60–5.29)
Erythrocyte rigidity index	4.59 (4.02–5.23)
Erythrocyte deformation index	0.82 (0.77–0.87)
Assigned viscosity, mPas	3.39 (3.03–3.78)
Fibrinogen, g/L	3.09 (2.97–3.15)
Whole blood high cut reduction viscosity	6.31 (5.56–7.22)
Whole blood high cut relative index	2.98 (2.67–3.33)
Whole blood low cut reduction viscosity	44.87 (41.02–48.39)
Plasma viscosity, mPas	1.41 (1.36–1.43)
Hematocrit, L/L	0.42 (0.40–0.46)

GWAS, genome-wide association study; IQR, interquartile range; BMI, body mass index.

increased erythrocytes aggregation, and decreased erythrocytes deformability. Hemorheological variations of the erythrocyte behavior and blood plasma can help in the clinical diagnosis [9].

Recently, the identification of various susceptibility loci and genes related to hematological traits in diverse ethnic groups may provide important insights into the hematology [10]. Christiansen et al. [11] have demonstrated that *ABO* locus was related to the increased platelet aggregation in patients with stable coronary artery disease. Krause et al. [12] reported that rs17114036, a common noncoding polymorphism at 1p32.2, is located in the endothelial enhancer dynamically regulated by hemodynamics. Seiki et al. [13] displayed the association of *ABO*, *PDGFRA-KIT*, *USP49-MED20-BSYL-CCND3*, *C6orf182-CD164*, *TERT*, and *TMPRSS6* variants with erythrocyte traits in Japanese population. Qayyum et al. [14] demonstrated that six single nucleotide polymorphisms (SNPs) were associated with platelet aggregation ($p < 5 \times 10^{-8}$). So far, although a number of loci associated with quantitative hematological traits have been discovered [15], genome-wide association studies (GWASs) for various hemorheological characteristics have not been reported. Therefore, it is necessary to determine the genetic variation related to hemorheological traits. Here, we performed a genome-wide association study to identify imputed genetic loci associated with hemorheological indexes in a cohort of healthy Chinese Han individuals by the Applied Biosystems Axiom™ Precision Medicine Diversity Array Chip.

Material and Method

Study Cohorts

A total of 838 participants (413 women and 425 men) visited the Health Care Center of Henan Provincial People's Hospital for annual checkup. All individuals were healthy Chinese Han population. Subjects with tumors, known disease, or pregnant women were excluded. To evaluate genetic association, 14 hemorheological indexes were examined (Table 1), including nd1 (mPas), nd30 (mPas), nd300 (mPas), relative index of whole blood hyposectomy, erythrocyte aggregation index, erythrocyte rigidity index, erythrocyte deformation index, assigned viscosity (mPas), fibrinogen (g/L), whole blood high cut reduction viscosity, whole blood high cut relative index, whole blood low cut reduction viscosity, plasma viscosity (mPas), and hematocrit (L/L). Demographic and hemorheology data were obtained from questionnaires or medical records. Written informed consent was obtained from all of the participating cohort. The protocols were approved by the Institutional Research Ethics Committee of Henan Provincial People's Hospital and complied with the Declaration of Helsinki.

GWAS Genotyping and Genotype Imputation

A peripheral blood sample (5 mL) of each participant was collected in EDTA-coated tubes, and genomic DNA was purified using the GoldMag DNA Isolation Kit (GoldMag Co., Ltd., Xi'an, China). A total of 796,288 loci were available for GWAS analysis based on the following: (1) sample calling rate >0.95, marker calling rate >0.90, and Hardy-Weinberg equilibrium $>5 \times 10^{-06}$ for quality control and (2) removing indels, copy number variation, duplication, and loci from sex chromosome. Genome-wide genotyping of the subjects was carried out using the Applied Biosystems Axiom™ Precision Medicine Diversity Array on the GeneTitanTM Multi-Channel Instrument (Thermo Fisher, CA, USA). Genotype clustering was conducted using Axiom Analysis Suite 6.0 software. Genome-wide data were imputed from the third phase of 1,000 genomes haplotype reference panels through IMPUTE2 software, and loci with minor allele frequency <1%, the correlation coefficient (r^2) linkage disequilibrium <0.5, and nonbiallelic were deleted. Taking into account the uncertainty of imputation, the association analysis was performed by Gold Helix SNP & Variation Suite 8.7 software. After quality control and imputation, 6,423,076 loci were included for final analysis.

Data Analysis

Continuous variables were evaluated for normality using the Kolmogorov-Smirnov test. Continuous variables with non-normal distribution as median with interquartile range were compared using the Mann-Whitney U test. Relations of SNPs to hemodynamic phenotypes were examined in the additive genetic model using mixed linear regression adjusting with age and gender by the PLINK software and combined with identical by descent matrix. The levels of hemodynamic indexes were normalized using rank-based inverse normal transformations. Manhattan plots and quantile-quantile plots were conducted by –log10 (p value) using R-package version 3.32. Locus regional plots were constructed by LocusZoom 1.1 software. The values of $p < 5 \times 10^{-8}$ means that the genetic polymorphism is genome-wide significantly associated with hemorheological indexes. The values of $p < 5 \times 10^{-6}$ suggests a suggestively significant genome-wide association with hemorheological indexes.

Bioinformatics Analysis

GWAS catalog (https://www.ebi.ac.uk/gwas/) and Clinvar (https://www.ncbi.nlm.nih.gov/clinvar/) were used to see if some of the SNPs were already associated with clinical phenotypes and

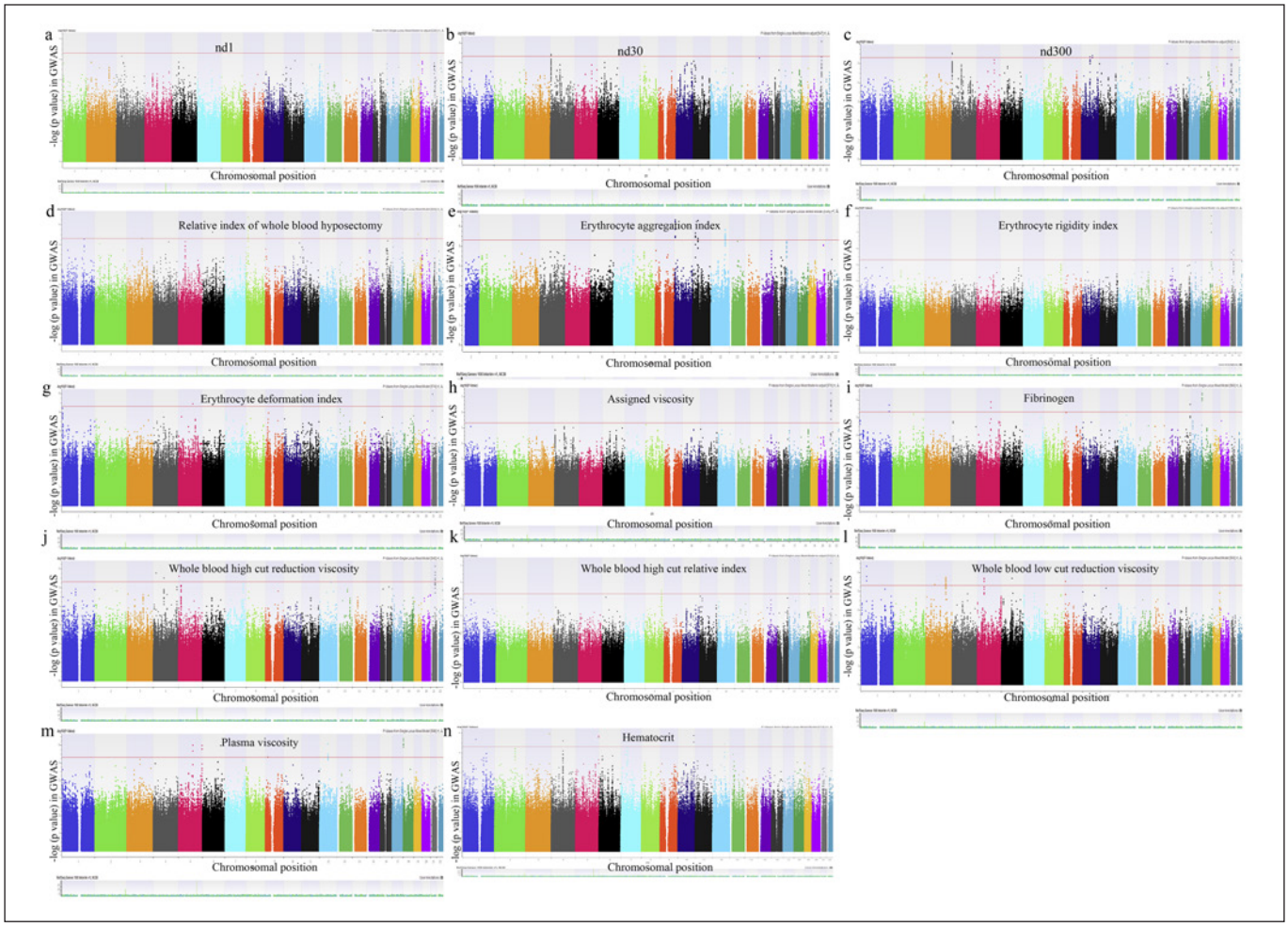

Fig. 1. a–n Manhattan plot for loci associated with levels of hemorheological indexes.

if these relate somehow to the parameters. HaploReg v4.1 database (https://pubs.broadinstitute.org/mammals/haploreg/haploreg.php) is a database used to predict the potential functions of selected SNPs.

Results

The Manhattan plot (Fig. 1) displayed the chromosome location of significantly associated loci with hemodynamic indexes, including nd1 (1 loci), nd30 (2 loci), nd300 (3 loci), relative index of whole blood hyposectomy (5 loci), erythrocyte aggregation index (4 loci), erythrocyte rigidity index (3 loci), erythrocyte deformation index (2 loci), assigned viscosity (1 loci), fibrinogen (4 loci), whole blood high cut reduction viscosity (5 loci), whole blood high cut relative index (3 loci), whole blood low cut reduction viscosity (6 loci), plasma viscosity (6 loci), and hematocrit (1 loci). A quantile-quantile plot for hemodynamic index levels is shown in Figure 2, and the distribution of p values for the association tests showed no evidence of systematic bias.

Table 2 displays the details of 38 loci with p values $<5 \times 10^{-6}$ for the levels of hemodynamic indexes. Of the 63 identified loci, *LOC730100* rs117580912 ($p = 9.56 \times 10^{-07}$) was associated with the nd1 level (online suppl. Fig. 1; see www.karger.com/doi/10.1159/000524849 for all online suppl. material). The significant association with nd30 concentration was for rs4689231 in *STK32B* ($p = 3.85 \times 10^{-06}$) and rs28371438 in *LOC102724502-OLIG2* ($p = 8.58 \times 10^{-07}$, online suppl. Fig. 2). Three SNPs (*STK32B* rs4689231: $p = 2.94 \times 10^{-06}$, *CCSER2-LINC01519* rs115646937: $p = 3.90 \times 10^{-06}$ and *LOC102724502-OLIG2* rs28371438: $p = 1.89 \times 10^{-06}$, respectively) were considered significant markers for nd300 level (online suppl. Fig. 3). Rs34469348 in *LSAMP* ($p = 4.87 \times 10^{-06}$), rs9361295 in *MEI4* ($p = 2.44 \times 10^{-06}$), rs2410367 in *TUSC3-MSR1* ($p = 4.24 \times 10^{-07}$), rs10977588 in *PTPRD* ($p = 2.88 \times 10^{-06}$), and rs745439 in *TSHZ3-THEG5* ($p = 3.14 \times 10^{-06}$) were associated with the level of the relative index of whole blood hyposectomy (online suppl. Fig. 4). The significant association with the concentration of erythrocyte aggregation index was for *SFMBT2* rs11255044 ($p = 4.83 \times$

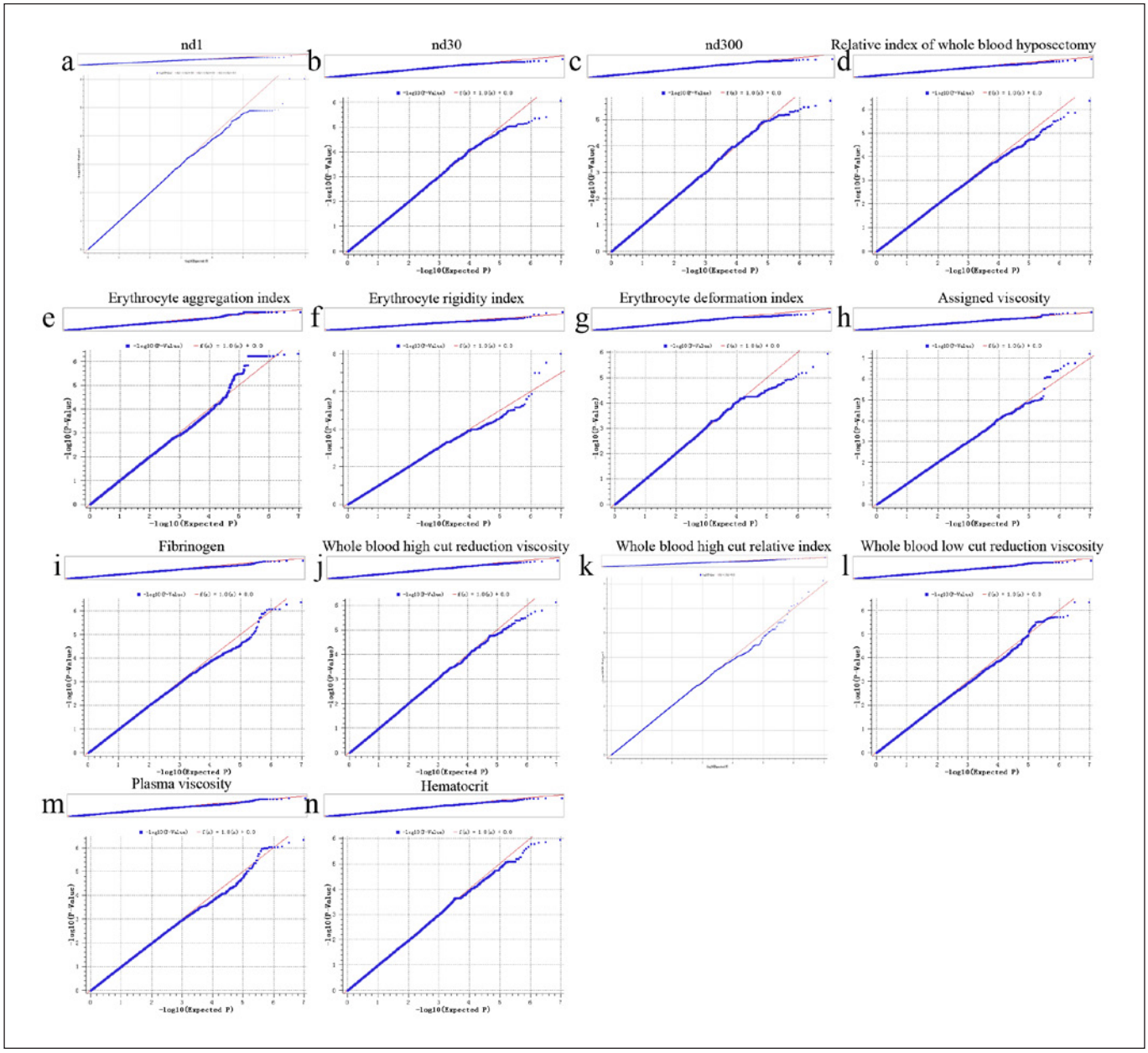

Fig. 2. a–n QQ plot for levels of hemorheological indexes. QQ, quantile-quantile.

10^{-07}), *LINC01493-LRRC4C* rs67538811 ($p = 5.21 \times 10^{-07}$), *NELL1-ANO5* rs12420881 ($p = 2.21 \times 10^{-06}$) and *C12orf42* rs56670740 ($p = 1.53 \times 10^{-06}$, online suppl. Fig. 5). Three genome-level significant SNPs (p value of 9.93×10^{-09} for rs11661911 in *GTSCR1-LINC01541*, 1.81×10^{-06} for rs1297329 in *USP25-MIR99AHG* and 1.29×10^{-06} for rs28371438 in *LOC102724502-OLIG2*) associated with erythrocyte rigidity index level were identified (online suppl. Fig. 6). We also found that *TMEM232* rs2900050 ($p = 3.72 \times 10^{-06}$) and *USP25-MIR99AHG* rs1297329 ($p = 1.14 \times 10^{-06}$) were significant loci for the circulating level of erythrocyte deformation index (online suppl. Fig. 7). Rs28371438 in *LOC102724502-OLIG2* ($p = 6.20 \times 10^{-08}$, online suppl. Fig. 8) was a significant marker related to the level of assigned viscosity. Four loci were associated with fibrinogen concentration, including rs78314456 in *CNIH3* ($p = 1.95 \times 10^{-06}$), rs3985087 in *TMEM232-SLC25A46* ($p = 1.31 \times 10^{-06}$), rs34247085 in *LINC00917-FENDRR* ($p = 1.80 \times 10^{-06}$), and rs9966987 in *LINC00470-METTL4* ($p = 4.29 \times 10^{-07}$, online suppl. Fig. 9). For whole blood high cut reduction viscosity, the significant association was with rs144907988 in *ADGRA3-GBA3* ($p = 1.74 \times 10^{-06}$), rs6827644 in *C4orf22* ($p = 3.18 \times 10^{-06}$), rs1030490 in *IRX1-LINC02114* ($p = 2.53 \times 10^{-06}$),

Transfus Med Hemother 2022;49:346–356
DOI: 10.1159/000524849

Table 2. Significant loci associated with hemorheology indexes from the GWAS cohorts

Characteristics	SNP ID	Chr	Position	REF/ ALT	SNP function	RefGene	MAF	β	SE	*p* value	GWAS catalog	HaploReg
nd1	rs117580912	2	51,343,364	C/T	ncRNA intronic	LOC730100	0.005	0.011	0.039	9.56E–07	–	Motifs changed
nd30	rs4689231	4	5,437,107	G/A	Intronic	STK32B	0.370	0.162	0.330	3.85E–06	–	Motifs changed
	rs28371438	21	32,986,517	C/T	Intergenic	LOC102724502;OLIG2	0.478	–0.231	0.331	8.58E–07	Height	Motifs changed
nd300	rs4689231	4	5,437,107	G/A	Intronic	STK32B	0.370	0.200	1.107	2.94E–06	–	Motifs changed
	rs115646937	10	84,813,648	A/G	Intergenic	CCSER2;LINC01519	0.092	–0.031	1.107	3.90E–06	–	Motifs changed
	rs28371438	21	32,986,517	C/T	Intergenic	LOC102724502;OLIG2	0.478	–0.193	1.107	1.89E–06	Height	Motifs changed
Relative index of whole blood hyposectomy	rs34469348	3	115,815,531	G/T	Intronic	LSAMP	0.094	–0.359	0.140	4.87E–06	–	Motifs changed
	rs9361295	6	77,831,550	C/A	Intronic	MEI4	0.259	–0.388	0.141	2.44E–06	–	Motifs changed
	rs2410367	8	15,931,636	T/C	Intergenic	TUSC3;MSR1	0.222	–0.194	0.140	4.24E–07	–	Motifs changed
	rs10977588	9	9,218,157	C/T	Intronic	PTPRD	0.010	–0.266	0.139	2.88E–06	–	Motifs changed
	rs745439	19	31,537,088	C/T	Intergenic	TSHZ3;THEG5	0.386	–0.450	0.143	3.14E–06	–	Motifs changed
Erythrocyte aggregation index	rs11255044	10	7,221,420	G/C	Intronic	SFMBT2	0.033	–0.063	1.433	4.83E–07	–	Motifs changed
	rs67538811	11	39,184,039	G/A	Intergenic	LINC01493;LRRC4C	0.140	0.030	1.436	5.21E–07	–	Motifs changed
	rs12420881	11	21,664,423	C/A	Intergenic	NELL1;ANO5	0.007	–0.006	1.433	2.21E–06	–	Motifs changed
	rs56670740	12	103,353,181	T/A	Intronic	C12orf42	0.247	–0.149	1.435	1.53E–06	–	Enhancer histone marks, motifs changed
Erythrocyte rigidity index	rs11661911	18	70,983,826	A/C	Intergenic	GTSCR1;LINC01541	0.135	–0.104	0.952	9.93E–09	–	Motifs changed
	rs1297329	21	15,939,669	G/A	Intergenic	USP25;MIR99AHG	0.013	–0.018	0.957	1.81E–06	–	Motifs changed
	rs28371438	21	32,986,517	C/T	Intergenic	LOC102724502;OLIG2	0.478	–0.220	0.958	1.29E–06	Height	Motifs changed
Erythrocyte deformation index	rs2900050	5	110,721,671	G/A	Intronic	TMEM232	0.008	0.092	0.998	3.72E–06	–	Motifs changed, selected eQTL hits
	rs1297329	21	15,939,669	G/A	Intergenic	USP25;MIR99AHG	0.013	0.057	0.996	1.14E–06	–	Motifs changed
Assigned viscosity	rs28371438	21	32,986,517	C/T	Intergenic	LOC102724502;OLIG2	0.479	–0.200	1.559	6.20E–08	Height	Motifs changed

Table 2 (continued)

Characteristics	SNP ID	Chr	Position	REF/ ALT	SNP function	RefGene	MAF	β	SE	*p* value	GWAS catalog	HaploReg
Fibrinogen	rs78314456	1	224,640,188	C/T	Intronic	CNIH3	0.008	−0.024	0.407	1.95E−06	–	Enhancer histone marks, DNAse, motifs changed
	rs3985087	5	110,736,955	C/A	Intergenic	TMEM232;SLC25A46	0.025	−0.052	0.407	1.31E−06	–	Promoter histone marks, enhancer histone marks, DNAse, proteins bound, motifs changed, selected eQTL hits
	rs34247085	16	86,472,977	G/A	Intergenic	LINC00917;FENDRR	0.008	0.033	0.408	1.80E−06	–	Enhancer histone marks, motifs changed
	rs9966987	18	1,918,849	C/A	Intergenic	LINC00470;METTL4	0.330	0.153	0.408	4.29E−07	–	Enhancer histone marks, motifs changed
Whole blood high cut reduction viscosity	rs144907988	4	22,589,091	C/T	Intergenic	ADGRA3;GBA3	0.002	−0.229	0.150	1.74E−06	–	–
	rs6827644	4	80,874,656	C/T	Intronic	C4orf22	0.066	−0.311	0.151	3.18E−06	–	Motifs changed
	rs1030490	5	4,574,832	T/G	Intergenic	IRX1;LINC02114	0.401	−0.037	0.156	2.53E−06	–	Motifs changed
	rs11911466	21	32,983,986	T/C	Intergenic	LOC102724502;OLIG2	0.416	−0.397	0.153	7.37E−07	–	Enhancer histone marks, motifs changed
	rs6519816	22	43,905,383	C/T	Intergenic	PNPLA5;PNPLA3	0.155	−0.165	0.151	3.37E−06	–	Enhancer histone marks, motifs changed
Whole blood high cut relative index	rs11990599	8	126,350,838	T/C	Intergenic	LOC101927657;FAM84B	0.120	−0.091	0.042	3.11E−06	–	Motifs changed
	rs11661911	18	70,983,826	A/C	Intergenic	GTSCR1;LINC01541	0.134	−0.105	0.043	2.09E−07	–	Motifs changed
	rs28371438	21	32,986,517	C/T	Intergenic	LOC102724502;OLIG2	0.479	−0.257	0.060	7.30E−08	Height	Motifs changed
Whole blood low cut reduction viscosity	rs2842173	1	43,493,328	T/C	Intergenic	SZT2;PTPRF	0.217	−0.280	0.159	4.56E−07	–	Enhancer histone marks, selected eQTL hits
	rs74525620	3	67,290,451	C/A	Intergenic	MIR4272;SUCLG2	0.003	−0.155	0.157	4.41E−06	–	Promoter histone marks, enhancer histone marks, motifs changed, selected eQTL hits
	rs73872706	3	151,645,475	G/C	Intergenic	MIR5186;AADACL2	0.138	−0.056	0.157	1.90E−06	–	Enhancer histone marks, motifs changed
	rs246509	5	52,968,323	A/C	Intergenic	ITGA1;ITGA2	0.219	−0.242	0.159	2.05E−06	–	Motifs changed, selected eQTL hits
	rs117016320	6	81,831,622	T/A	Intergenic	LINC01526;IBTK	0.012	−0.142	0.157	2.09E−06	–	Promoter histone marks, enhancer histone marks, DNAse, proteins bound, motifs changed
	rs10977641	9	9,291,862	A/G	Intronic	PTPRD	0.009	−0.140	0.157	3.02E−06	–	Motifs changed

Transfus Med Hemother 2022;49:346–356
DOI: 10.1159/000524849

Table 2 (continued)

Characteristics	SNP ID	Chr	Position	REF/ ALT	SNP function	RefGene	MAF	β	SE	*p* value	GWAS catalog	HaploReg
Plasma viscosity	rs3985087	5	110,736,955	C/A	Intergenic	TMEM232;SLC25A46	0.025	–0.048	0.917	1.01E–06	–	Promoter histone marks, enhancer histone marks, DNAse, proteins bound, motifs changed, selected eQTL hits
	rs118096558	5	180,197,694	G/A	Intronic	RASGEF1C	0.009	–0.016	0.917	1.06E–06	–	Enhancer histone marks, motifs changed
	rs11794922	9	18,789,607	T/G	Intronic	ADAMTSL1	0.002	–0.029	0.917	4.96E–06	–	Enhancer histone marks, motifs changed
	rs76126204	12	64,983,618	C/T	ncRNA intronic	LINC02231	0.030	0.076	0.919	8.66E–07	–	Motifs changed
	rs9966987	18	1,918,849	C/A	Intergenic	LINC00470;METTL4	0.269	0.093	0.917	4.59E–07	–	Enhancer histone marks, motifs changed
	rs140700208	6	139,497,581	T/C	Intergenic	LINC01625;LOC100132735	0.331	0.160	0.917	1.06E–06	–	Promoter histone marks, enhancer histone marks, DNAse, proteins bound, motifs changed
Hematocrit	rs78577937	4	92,146,844	A/C	Intergenic	CCSER1;LNCPRESS2	0.168	–0.509	0.135	1.43E–06	–	–

GWAS, genome-wide association study; SNP, single nucleotide polymorphism; REF/ALT, reference/alternates; MAF, minor allele frequency.

rs11911466 in *LOC102724502-OLIG2* ($p = 7.37 \times 10^{-07}$), and rs6519816 in *PNPLA5-PNPLA3* ($p = 3.37 \times 10^{-06}$, online suppl. Fig. 10). Rs11990599 in *LOC101927657-FAM84B* ($p = 3.11 \times 10^{-06}$), rs11661911 in *GTSCR1-LINC01541* ($p = 2.09 \times 10^{-07}$), and rs28371438 in *LOC102724502-OLIG2* ($p = 7.30 \times 10^{-08}$, online suppl. Fig. 11) were related to the level of whole blood high cut relative index. Six SNPs also achieved significant association with the level of whole blood low cut reduction viscosity, with p values of 4.56×10^{-07}, 4.41×10^{-06}, 1.90×10^{-06}, 2.05×10^{-06}, 2.09×10^{-06}, and 3.02×10^{-06} for *SZT2-PTPRF* rs2842173, *MIR4272-SUCLG2* rs74525620, *MIR5186-AADACL2* rs73872706, *ITGA1-ITGA2* rs246509, *LINC01526-IBTK* rs117016320, and *PTPRD* rs10977641, respectively (online suppl. Fig. 12). Rs3985087 in *TMEM232-SLC25A46* ($p = 1.01 \times 10^{-06}$), rs118096558 in *RASGEF1C* ($p = 1.06 \times 10^{-06}$), rs11794922 in *ADAMTSL1* ($p = 4.96 \times 10^{-06}$), rs76126204 in *LINC02231* ($p = 8.66 \times 10^{-07}$), rs9966987 in *LINC00470-METTL4* ($p = 4.59 \times 10^{-07}$), and rs140700208 in *LINC01625-LOC100132735* ($p = 1.06 \times 10^{-06}$) showed suggestive associations with the level of plasma viscosity (online suppl. Fig. 13). Moreover, the significant association of hematocrit was with rs78577937 in the intergenic region of the *CCSER1-LNCPRESS2* gene ($p = 1.43 \times 10^{-06}$, online suppl. Fig. 14).

Based on GWAScat database (Table 2), we found that rs28371438 was associated with height trait. The results of HaploReg v4.1 displayed that these SNPs were associated with the regulation of promoter and/or enhancer histones, DNAse, changed motifs, and selected eQTL hits.

Discussion

Hemorheology (also named blood rheology) is the study of the flow characteristics of blood and its elements. Hemorheology indicators, such as whole blood viscosity, plasma viscosity, erythrocyte aggregation, erythrocyte rigidity, erythrocyte deformation, fibrinogen, and hematocrit, play fundamental roles in maintaining microcirculation [16, 17]. In our study of 14 hemorheological traits, a total of 38 SNPs were significantly related to hemorheological traits ($p < 5 \times 10^{-6}$). In which, six SNPs, including rs28371438 for nd30, nd300, erythrocyte rigidity index, assigned viscosity and whole blood high cut relative index; rs4689231 of *STK32B* for nd30 and nd300; rs11661911 for erythrocyte rigidity index and whole blood high cut relative index; rs1297329 for erythrocyte rigidity index and erythrocyte deformation index; rs3985087 and rs9966987 for fibrinogen and plasma viscosity, were identified as multiple hematological markers. This is the first GWAS examining the genetic loci of hemorheological indexes in a normal Chinese Han population.

Blood viscosity and its major determinants (hematocrit and plasma viscosity) are related to increased risks of cardiovascular disease and cardiovascular-related premature mortality [16]. In our study, *LOC730100* rs117580912 was associated with the nd1 level. *LOC730100* on chromosome 2p16.3 was increased expression in glioma tissues and cell lines, and enhanced proliferation and invasion of glioma cells [18]. The significant association with nd30 and nd300 levels was for *STK32B* rs4689231 and *LOC102724502-OLIG2* rs28371438. *CCSER2-LINC01519* rs115646937 was also a significant marker for the nd300 level. The effects of overexpressed *STK32B* (chromosome 4p16.2) might be involved in relevant essential tremor pathways [19]. *OLIG2*, located on chromosome 21q22.11, is the key transcription factor that maintains the neural progenitor cells of the pMN domain [20]. *CCSER2* on chromosome 10q23.1 was identified a reference gene, also called novel housekeeping gene [21].

Moreover, rs28371438 in *LOC102724502-OLIG2*, rs3985087 in *TMEM232-SLC25A46*, rs118096558 in *RASGEF1C*, rs11794922 in *ADAMTSL1*, rs76126204 in *LINC02231*, rs9966987 in *LINC00470-METTL4*, and rs140700208 in *LINC01625-LOC100132735* showed suggestive associations with the level of plasma viscosity. *TMEM232* associated with atopic dermatitis in the Chinese Han population [22] and *SLC25A46* related to patients with Parkinson's disease and optic atrophy [23] are located on chromosome 5q22.1. *ADAMTSL1* (chromosome 9p22.2-p22.1) protein was lower expressed in intracranial aneurysm tissue than in the control cerebral artery [24]. LINC00470 (chromosome 18p11.32) promoted the proliferation and invasion of glioma cell by LINC00470/miR-134/Myc/ABCC1 axis [25]. *METTL4*, located on chromosome 18p11.32, was identified as a candidate of N6-adenine methylase [26]. The function of long intergenic nonprotein coding RNA (LOC102724502, LINC01519, LINC02231, LINC01625, and LOC100132735) and RASGEF1C needs further study.

Hematocrit and fibrinogen are important determinants of whole blood viscosity. McMullin et al. reported that red cell mass measurement along with hemoglobin and hematocrit cut-offs as a major diagnostic criterion for the diagnosis of polycythemia Vera [27]. In this study, the significant association of hematocrit was with rs78577937 in the intergenic region of *CCSER1-LNCPRESS2*. *CCSER1* (chromosome 4q22.1), also known as *FAM190A*, was reported to be associated with type 1 diabetes [28]. LNCPRESS2 is a long intergenic nonprotein coding RNA, whose function needs further study. Fibrinogen is an acute phase protein with proinflammatory and anti-inflammatory properties. Its secretion in the liver is upregulated during inflammation [29]. Previous study has shown that elevated fibrinogen is associated with an increased risk of lung, colorectal, and breast cancers [30].

Four loci were associated with fibrinogen concentration, including *CNIH3* rs78314456, *TMEM232-SLC25A46* rs3985087, *LINC00917-FENDRR* rs34247085, and *LINC00470-METTL4* rs9966987. Cornichon 3 (*CNIH3*, chromosome 1q42.12) enhanced the glutamate sensitivity, single-channel conductance, and calcium permeability of CP-AMPARs while decreasing their block by intracellular polyamines [31]. *FENDRR* (chromosome 16q24.1) is lower expressed in colorectal cancer tissue and cells, which is responsible for inhibiting of cell proliferation, migration, and invasion [32].

The aggregation of red blood cells may be enhanced during various pathophysiological processes, including circulatory and metabolic disorders, infection, blood pathology, and several other disease states [33]. Altered erythrocyte aggregation may be a factor that affects the clinical process and also an indicator for the development and prognosis of disease. We found that the significant association with the concentration of erythrocyte aggregation index was for *SFMBT2* rs11255044, *LINC01493-LRRC4C* rs67538811, *NELL1-ANO5* rs12420881, and *C12orf42* rs56670740. *SFMBT2*, a circRNA located on chromosome 10p14, had an increased expression level in gastric cancer tissues and was associated with the proliferation of gastric cancer cells [34]. *LRRC4C* (chromosome 11p12) was a novel candidate susceptibility gene for pediatric central nervous system tumors [35]. *NELL1* (chromosome 11p15.1) was associated with bone formation and osteoclast differentiation [36], and *ANO5* (chromosome 11p15.1) was related to myopathy. Hypothetical gene *C12orf42*, located on chromosome 12q23.2-q23.3, was associated with T-lymphoblastic lymphoma [37].

Erythrocyte aggregation is reversible and shear-dependent (i.e., disperses at high shear and reforms at low shear), and the degree of erythrocyte aggregation is the main determinant of low-shear blood viscosity [33]. Our study displayed that *LSAMP* rs34469348, *MEI4* rs9361295, *TUSC3-MSR1* rs2410367, *PTPRD* rs10977588, and *TSHZ3-THEG5* rs745439 were associated with the level of relative index of whole blood hyposectomy. Rs11990599 in *LOC101927657-FAM84B*, rs11661911 in *GTSCR1-LINC01541*, and rs28371438 in *LOC102724502-OLIG2* were related to the level of whole blood high cut relative index. For whole blood high cut reduction viscosity, the significant association was with *ADGRA3-GBA3* rs144907988, *C4orf22* rs6827644, *IRX1-LINC02114* rs1030490, *LOC102724502-OLIG2* rs11911466, and *PNPLA5-PNPLA3* rs6519816. Six SNPs also achieved the significant association with the level of whole blood low cut reduction viscosity for *SZT2-PTPRF* rs2842173, *MIR4272-SUCLG2* rs74525620, *MIR5186-AADACL2* rs73872706, *ITGA1-ITGA2* rs246509, *LINC01526-IBTK* rs117016320, and *PTPRD* rs10977641, respectively.

The rigidity of erythrocyte is the main rheological characteristic of the blood of Sickle Cell Anemia patients and several pathologies [38]. Three genome-level significant SNPs (rs11661911 in *GTSCR1-LINC01541*, rs1297329 in *USP25-MIR99AHG* and rs28371438 in *LOC102724502-OLIG2*) associated with erythrocyte rigidity index level were identified. *LINC01541* (chromosome 18q22.3) plays a key role in 17β-estradiol (17β-E2)-stimulated endometrial stromal cells [39]. *USP25* (chromosome 21q21.1) suppresses the degradation of BCR-ABL protein in cells harboring the Philadelphia chromosome (Ph) in chronic myelogenous leukemia [40]. LncRNA host gene *MIR99AHG* (alias *MONC*) interfered with hematopoietic lineage decisions and enhanced the proliferation of immature erythroid progenitor cells in acute megakaryoblastic leukemia [41]. Erythrocyte deformation is determined mainly by the fluidity of the membrane and the viscosity of the cytoplasm, but extracellular factors may have an irreversible effect on the erythrocyte membrane [42]. Fornal et al. [43] reported a statistically significant correlation between left ventricular mass index, erythrocyte deformability, and aggregability. We also found that *TMEM232* rs2900050 and *USP25-MIR99AHG* rs1297329 were significant loci for the circulating level of erythrocyte deformation index.

Several potential limitations of this study cannot be ignored. First, all subjects were recruited from the same hospital; therefore, there was selection bias. Second, all participants were only from populations of Chinese Han ancestry, suggesting our finding couldn't be generalized to other ethnic groups. Therefore, replication studies in other Chinese Han populations or other ethnic groups are required to confirm the association of the identified loci with hemorheological phenotypes. Third, the potential function of identified loci has not been assessed. Further functional analysis is required to reveal the biological mechanism behind the observed associations. Four, the most commonly accepted threshold of a genome-wide association study is $p < 5 \times 10^{-8}$. After consulting the literature on disease GWAS, we found that when the sample size is small, a relatively relaxed threshold will be selected [44–46]. Therefore, we chose a relatively relaxed threshold as the suggestive threshold for significant genome-wide association ($p < 5 \times 10^{-6}$). However, to the best of our knowledge, this is the first GWAS examining the genetic loci of hemorheological indexes in a normal Chinese Han population. The identification of susceptibility loci and genes related to hemorheological indexes may provide important insight into the regulation of hemorheological indexes.

Conclusion

In summary, we reported 38 suggestive loci associated with hemorheological indexes in the Chinese Han population. In particular, six SNPs (rs28371438 in *LOC102724502-OLIG2*, rs4689231 of STK32B, rs11661911 in *GTSCR1-LINC01541*, rs1297329 in *USP25-MIR99AHG*, rs3985087 in *TMEM232-SLC25A46*, rs9966987 in *LINC00470-METTL4*) were identified as multiple hematological markers. The results of our genome-wide association study may represent biological candidates for hemorheological indexes and contribute to hemorheological study.

Statement of Ethics

Written informed consent was obtained from all of the participating cohort. The protocols were approved by the Institutional Research Ethics Committee of Henan Provincial People's Hospital and complied with the Declaration of Helsinki.

Conflict of Interest Statement

The authors declare that they have no conflict of interest.

Funding Sources

This work was supported by the National Key Research and Development Program comes from the Ministry of Science and Technology, PRC (Project number: 2018YFC0114502).

Author Contributions

Yuxiao Sun drafted the work or revised it critically for important content; Zhaoyun Cheng, Zhiping Guo, and Guoyou Dai performed the experiments; Yongqiang Li, Yan Chen, and Ruigang Xie analyzed the data; Xianqing Wang, Mingxia Cui, Guoqing Lu, and Aifeng Wang collected the samples and information. Chuanyu Gao conceived and designed the experiments. All the authors have read and approved the manuscript.

Data Availability Statement

All data generated or analyzed during this study are included in this article and its online supplementary material. Anyone who is interested in the information should contact the corresponding author.

References

1 Caprari P, Massimi S, Diana L, Sorrentino F, Maffei L, Materazzi S, et al. Hemorheological alterations and oxidative damage in sickle cell anemia. Front Mol Biosci. 2019;6:142.
2 Lee H, Na W, Lee SB, Ahn CW, Moon JS, Won KC, et al. Potential diagnostic hemorheological indexes for chronic kidney disease in patients with type 2 diabetes. Front Physiol. 2019;10:1062.
3 Baskurt OK, Meiselman HJ. Blood rheology and hemodynamics. Semin Thromb Hemost. 2003;29(5):435–50.
4 Stoltz JF. Hemorheology: pathophysiological significance. Acta Med Port. 1985;6(7–8):S4–13.
5 Javadi E, Jamali S. Hemorheology: the critical role of flow type in blood viscosity measurements. Soft Matter. 2021;17(37):8446–58.
6 Wiewiora M, Piecuch J, Glűck M, Slowinska-Lozynska L, Sosada K. The effects of weight loss surgery on blood rheology in severely obese patients. Surg Obes Relat Dis. 2015;11(6):1307–14.
7 Peng WK, Chen L, Boehm BO, Han J, Loh TP. Molecular phenotyping of oxidative stress in diabetes mellitus with point-of-care NMR system. NPJ Aging Mech Dis. 2020;6:11.
8 Ritchie SA, Connell JM. The link between abdominal obesity, metabolic syndrome and cardiovascular disease. Nutr Metab Cardiovasc Dis. 2007;17(4):319–26.
9 Yeom E, Lee SJ. Microfluidic-based speckle analysis for sensitive measurement of erythrocyte aggregation: a comparison of four methods for detection of elevated erythrocyte aggregation in diabetic rat blood. Biomicrofluidics. 2015;9(2):024110.
10 Yasukochi Y, Sakuma J, Takeuchi I, Kato K, Oguri M, Fujimaki T, et al. Identification of nine novel loci related to hematological traits in a Japanese population. Physiol Genomics. 2018;50(9):758–69.
11 Christiansen MK, Larsen SB, Nyegaard M, Neergaard-Petersen S, Würtz M, Grove EL, et al. The ABO locus is associated with increased platelet aggregation in patients with stable coronary artery disease. Int J Cardiol. 2019;286:152–8.
12 Krause MD, Huang RT, Wu D, Shentu TP, Harrison DL, Whalen MB, et al. Genetic variant at coronary artery disease and ischemic stroke locus 1p32.2 regulates endothelial responses to hemodynamics. Proc Natl Acad Sci U S A. 2018;115(48):E11349–58.
13 Seiki T, Naito M, Hishida A, Takagi S, Matsunaga T, Sasakabe T, et al. Association of genetic polymorphisms with erythrocyte traits: verification of SNPs reported in a previous GWAS in a Japanese population. Gene. 2018;642:172–7.
14 Qayyum R, Becker LC, Becker DM, Faraday N, Yanek LR, Leal SM, et al. Genome-wide association study of platelet aggregation in African Americans. BMC Genet. 2015;16:58.
15 Okada Y, Kamatani Y. Common genetic factors for hematological traits in humans. J Hum Genet. 2012;57(3):161–9.
16 Peters SA, Woodward M, Rumley A, Tunstall-Pedoe HD, Lowe GD. Plasma and blood viscosity in the prediction of cardiovascular disease and mortality in the Scottish Heart Health Extended Cohort Study. Eur J Prev Cardiol. 2017;24(2):161–7.
17 Schmid-Schönbein H. Microrheology of erythrocytes, blood viscosity, and the distribution of blood flow in the microcirculation. Int Rev Physiol. 1976;9:1–62.
18 Li Q, Lu J, Xia J, Wen M, Wang C. Long noncoding RNA LOC730100 enhances proliferation and invasion of glioma cells through competitively sponging miR-760 from FOXA1 mRNA. Biochem Biophys Res Commun. 2019;512(3):558–63.
19 Liao C, Sarayloo F, Vuokila V, Rochefort D, Akçimen F, Diamond S, et al. Transcriptomic changes resulting from STK32B overexpression identify pathways potentially relevant to essential tremor. Front Genet. 2020;11:813.
20 Li H, de Faria JP, Andrew P, Nitarska J, Richardson WD. Phosphorylation regulates OLIG2 cofactor choice and the motor neuron-oligodendrocyte fate switch. Neuron. 2011;69(5):918–29.
21 Tilli TM, Castro S, Tuszynski JA, Carels N. A strategy to identify housekeeping genes suitable for analysis in breast cancer diseases. BMC genomics. 2016;17(1):639.
22 Wu YY, Tang JP, Liu Q, Zheng XD, Fang L, Yin XY, et al. Scanning indels in the 5q22.1 region and identification of the TMEM232 susceptibility gene that is associated with atopic dermatitis in the Chinese Han population. Gene. 2017;617:17–23.

23 Bitetto G, Malaguti MC, Ceravolo R, Monfrini E, Straniero L, Morini A, et al. SLC25A46 mutations in patients with Parkinson's disease and optic atrophy. Parkinsonism Relat Disord. 2020;74:1–5.
24 Chen S, Li M, Xin W, Liu S, Zheng L, Li Y, et al. Intracranial aneurysm's association with genetic variants, transcription abnormality, and methylation changes in ADAMTS genes. PeerJ. 2020;8:e8596.
25 Wu C, Su J, Long W, Qin C, Wang X, Xiao K, et al. LINC00470 promotes tumour proliferation and invasion, and attenuates chemosensitivity through the LINC00470/miR-134/Myc/ABCC1 axis in glioma. J Cell Mol Med. 2020;24(20):12094–106.
26 Zhang Z, Hou Y, Wang Y, Gao T, Ma Z, Yang Y, et al. Regulation of adipocyte differentiation by METTL4, a 6 mA methylase. Sci Rep. 2020;10(1):8285.
27 McMullin MF, Reilly JT, Campbell P, Bareford D, Green AR, Harrison CN, et al. Amendment to the guideline for diagnosis and investigation of polycythaemia/erythrocytosis. Br J Haematol. 2007;138(6):821–2.
28 Haukka J, Sandholm N, Valo E, Forsblom C, Harjutsalo V, Cole JB, et al. Novel linkage peaks discovered for diabetic nephropathy in individuals with type 1 diabetes. Diabetes. 2021;70(4):986–95.
29 Kawada T. Relationships between the smoking status and plasma fibrinogen, white blood cell count and serum C-reactive protein in Japanese workers. Diabetes Metab Syndr. 2015;9(3):180–2.
30 Allin KH, Bojesen SE, Nordestgaard BG. Inflammatory biomarkers and risk of cancer in 84,000 individuals from the general population. Int J Cancer. 2016;139(7):1493–500.
31 Coombs ID, Soto D, Zonouzi M, Renzi M, Shelley C, Farrant M, et al. Cornichons modify channel properties of recombinant and glial AMPA receptors. J Neurosci. 2012;32(29):9796–804.
32 Cheng C, Li H, Zheng J, Xu J, Gao P, Wang J. FENDRR sponges miR-424-5p to inhibit cell proliferation, migration and invasion in colorectal cancer. Technol Cancer Res Treat. 2020;19:1533033820980102.
33 Baskurt OK, Meiselman HJ. Erythrocyte aggregation: basic aspects and clinical importance. Clin Hemorheol Microcirc. 2013;53(1–2):23–37.
34 Sun H, Xi P, Sun Z, Wang Q, Zhu B, Zhou J, et al. Circ-SFMBT2 promotes the proliferation of gastric cancer cells through sponging miR-182-5p to enhance CREB1 expression. Cancer Manag Res. 2018;10:5725–34.
35 Foss-Skiftesvik J, Hagen CM, Mathiasen R, Adamsen D, Bækvad-Hansen M, Børglum AD, et al. Genome-wide association study across pediatric central nervous system tumors implicates shared predisposition and points to 1q25.2 (PAPPA2) and 11p12 (LRRC4C) as novel candidate susceptibility loci. Childs Nerv Syst. 2020;37(3):819–30.
36 Li C, Zheng Z, Ha P, Jiang W, Berthiaume EA, Lee S, et al. Neural EGFL like 1 as a potential pro-chondrogenic, anti-inflammatory dual-functional disease-modifying osteoarthritis drug. Biomaterials. 2020;226:119541.
37 Przybylski GK, Dittmann K, Grabarczyk P, Dölken G, Gesk S, Harder L, et al. Molecular characterization of a novel chromosomal translocation t(12;14)(q23;q11.2) in T-lymphoblastic lymphoma between the T-cell receptor delta-deleting elements (TRDREC and TRAJ61) and the hypothetical gene C12orf42. Eur J Haematol. 2010;85(5):452–6.
38 Valadão Cardoso A. An experimental erythrocyte rigidity index (Ri) and its correlations with Transcranial Doppler velocities (TAMMV), Gosling Pulsatility Index PI, hematocrit, hemoglobin concentration and red cell distribution width (RDW). PLoS One. 2020;15(2):e0229105.
39 Mai H, Xu H, Lin H, Wei Y, Yin Y, Huang Y, et al. LINC01541 functions as a ceRNA to modulate the Wnt/β-catenin pathway by decoying miR-506-5p in endometriosis. Reprod Sci. 2020;28(3):665–74.
40 Shibata N, Ohoka N, Tsuji G, Demizu Y, Miyawaza K, Ui-Tei K, et al. Deubiquitylase USP25 prevents degradation of BCR-ABL protein and ensures proliferation of Ph-positive leukemia cells. Oncogene. 2020;39(19):3867–78.
41 Emmrich S, Streltsov A, Schmidt F, Thangapandi VR, Reinhardt D, Klusmann JH. LincRNAs MONC and MIR100HG act as oncogenes in acute megakaryoblastic leukemia. Mol Cancer. 2014;13:171.
42 Radosinska J, Vrbjar N. The role of red blood cell deformability and Na,K-ATPase function in selected risk factors of cardiovascular diseases in humans: focus on hypertension, diabetes mellitus and hypercholesterolemia. Physiol Res. 2016;65(Suppl 1):S43–54.
43 Fornal M, Korbut RA, Królczyk J, Grodzicki T. Left ventricular geometry and rheological properties of erythrocytes in patients at cardiovascular disease risk. Clin Hemorheol Microcirc. 2009;43(3):203–8.
44 de Vries PS, Brown MR, Bentley AR, Sung YJ, Winkler TW, Ntalla I, et al. Multiancestry genome-wide association study of lipid levels incorporating gene-alcohol interactions. Am J Epidemiol. 2019;188(6):1033–54.
45 Sim X, Ong RT, Suo C, Tay WT, Liu J, Ng DP, et al. Transferability of type 2 diabetes implicated loci in multi-ethnic cohorts from Southeast Asia. PLoS Genet. 2011;7(4):e1001363.
46 Gallois A, Mefford J, Ko A, Vaysse A, Julienne H, Ala-Korpela M, et al. A comprehensive study of metabolite genetics reveals strong pleiotropy and heterogeneity across time and context. Nat Commun. 2019;10(1):4788.